ANALYSIS AND FINITE ELEMENT SIMULATION OF MHD FLOWS, WITH AN APPLICATION TO LIQUID METAL PROCESSING [1]

A. J. Meir and Paul G. Schmidt

Department of Mathematics
Auburn University, AL 36849-5310, USA

Abstract

We present a novel approach to the mathematical analysis and computational simulation of fully three-dimensional, nonlinear, viscous, incompressible MHD flow in complex configurations involving several liquid and solid conductors. Such configurations arise in numerous metallurgical processes. Employing the current density rather than the magnetic field as the primary electromagnetic variable, it is possible to avoid artificial or highly idealized boundary conditions for electric and magnetic fields and to account exactly for the electromagnetic interaction of the flow region with the surrounding space. In addition, the approach lends itself naturally to finite-element based discretization techniques. As an application, we simulate the stationary flow of an electrically conducting fluid around a solid spherical particle of arbitrary conductivity, in the presence of crossed uniform electric and magnetic fields, and compute the Lorentz, pressure, and viscous forces exerted on the particle. This problem arises in connection with the electromagnetic filtration (purification) of molten metals before the casting stage.

---

[1] This material is based upon work supported by the National Science Foundation under Grants DMS-9404440 and DMS-9625096.

Introduction

Numerous metallurgical processes are governed by MHD effects resulting from the macroscopic interaction of liquid metals with applied or induced currents, electric and magnetic fields. Frequently these effects are technologically exploited in order to drive or to control the flow of metallic melts. Typical examples include the electromagnetic stirring of molten metals before the casting stage [1]; electromagnetic turbulence control in induction furnaces [2]; electromagnetic damping of buoyancy-driven flow during solidification [3]; and the electromagnetic shaping of ingots in continuous casting [4].

Another application, which has recently garnered much attention, is the electromagnetic filtration (purification) of metal alloys [5–7]. While classical methods for the removal of impurities, such as gravity sedimentation/flotation or centrifugation, rely on *density differences* between the unwanted inclusions and the metallic melt, electromagnetic filtration techniques exploit *conductivity differences* between inclusions and melt. If, for example, a steady, uniform current $\mathbf{J}_0$ is passed through the melt and crossed with a steady, uniform magnetic field $\mathbf{B}_0$, then the resulting Lorentz forces will accelerate an immersed particle (of electrical conductivity σ_p) relative to the surrounding fluid (of electrical conductivity σ_f) provided that $\sigma_p \neq \sigma_f$.

In the simplest case, if induction effects are negligible and the geometric configuration is such that the presence of the inclusion does not distort the current stream lines and the melt remains at rest, then the current density in the particle is $\sigma_p/\sigma_f \mathbf{J}_0$, the resultant force (per unit volume) experienced by the particle is $(\sigma_p/\sigma_f - 1)\mathbf{J}_0 \times \mathbf{B}_0$, and the particle will migrate in a direction perpendicular to both $\mathbf{J}_0$ and $\mathbf{B}_0$. In general, however, the situation is much more complex: The presence of the inclusion will distort the current stream lines, leading to rotational Lorentz forces that cannot be balanced by pressure gradients only; as a consequence the melt will be set in motion. In addition, induction effects may significantly alter the applied force field.

Successful industrial application of electromagnetic filtration techniques requires a thorough qualitative and quantitative understanding of the underlying MHD phenomena. Analytical and numerical models are needed to predict the current distribution, the structure of the flow field, and the forces acting on immersed particles (Lorentz, pressure, and viscous forces). Since the governing equations are genuinely nonlinear, explicit solutions or asymptotic expansions are feasible only in idealized situations where symmetries and/or asymptotic values of characteristic flow parameters (Reynolds number, Hartmann number, etc.) effectively reduce the problem to a linear one. Much has been achieved in this arena over the past decade. See, for example, [8–10] for detailed and insightful theoretical investigations of MHD flow around solid cylindrical, liquid spherical, and solid spherical inclusions, respectively, in the presence of crossed uniform electric and magnetic fields. A different technique, employing alternating currents induced by a time-varying magnetic field, is analyzed in [11].

While explicit solutions and asymptotic expansions in special situations have greatly enhanced the theoretical understanding of electromagnetic filtration processes, the general, nonlinear, fully three-dimensional case appears to be tractable only by way of direct numerical simulation. The same goes without saying for numerous other MHD-dominated metallurgical processes such as those mentioned at the beginning. Common features, shared by all those processes, include complex, three-dimensional geometry and the nonlinear interaction of several subsystems. All are governed by the Navier-Stokes equations, posed in the regions occupied by electrically conducting fluids; Ohm's law, valid in the fluid regions as well as in immersed or adjacent solid conductors; and Maxwell's equations, which hold throughout space. At interfaces separating media with different rheological and electromagnetic properties, flow velocities, current densities, and electric and magnetic fields will typically satisfy jump conditions or continuity relations rather than standard-type boundary conditions.

In the sequel, we will outline a novel analytical and computational approach to the MHD equations, which permits (at least in principle) the solution of a wide variety of highly complex MHD flow problems involving several fluid or solid conductors in arbitrary three-dimensional geometries. One key idea is to employ the current density (rather than the magnetic field) as the primary electromagnetic variable. This allows us to avoid artificial or highly idealized boundary conditions for the electric and magnetic fields and to confine virtually all computations to the bounded region of space occupied by fluid and solid conductors with unknown current distribution, while still accounting exactly for the electromagnetic interaction of these conductors with the surrounding space. Similar ideas have been exploited, both analytically and numerically, in [12–13], although in a much less general setting.

As an application of the method, we describe a direct numerical simulation of fully three-dimensional, nonlinear MHD flow around a solid spherical inclusion of arbitrary conductivity in the presence of crossed uniform electric and magnetic fields (a problem with direct bearing on the theory of electromagnetic filtration). We describe several computer experiments that illustrate, despite their somewhat academic nature, the feasibility of our approach in dealing with realistic MHD flow problems in metallurgy.

The MHD Equations: A General Framework

MHD-dominated processes in metallurgy typically involve a variety of conductors, each of which is either a solid or a viscous, incompressible fluid. Let Ω denote the union of all conducting regions, solid or fluid, where the current density $\mathbf{J}$ is unknown. In addition, there may be external conductors carrying given, externally maintained currents $\mathbf{J}_{ext}$. Let Ω_f denote the subset of Ω occupied by conducting fluids, where both $\mathbf{J}$ and the flow velocity $\mathbf{u}$ must be determined. Technically, both Ω and Ω_f are assumed to be bounded, open, generally disconnected subsets of $\mathbb{R}^3$, with sufficiently regular (at least Lipschitz continuous) boundaries $\partial\Omega$ and $\partial\Omega_f$, respectively.

The motion of the fluids in Ω_f is governed by the Navier-Stokes equations:

$$\rho\mathbf{u}_t - \eta\Delta\mathbf{u} + \rho(\mathbf{u}\cdot\nabla)\mathbf{u} + \nabla p - \mathbf{J}\times\mathbf{B} = \mathbf{F}_0 \quad \text{and} \quad \nabla\cdot\mathbf{u} = 0 \quad \text{in } \Omega_f. \tag{1}$$

Here $\mathbf{u}$ and p denote the velocity field and scalar pressure, $\mathbf{J}$ and $\mathbf{B}$ the current density and magnetic flux density, respectively. The term $\mathbf{J}\times\mathbf{B}$ represents the Lorentz force, the right-hand side $\mathbf{F}_0$ is a given body force (such as gravity). The density ρ and viscosity η are assumed to be constant in each of the fluids involved (that is, in each of the connected components of Ω_f), but with possibly different values in different fluids (that is, in different components of Ω_f). The equations (1) must be supplemented by suitable boundary and initial conditions, for example,

$$\mathbf{u} = \mathbf{g} \quad \text{on } \partial\Omega_f \quad \text{and} \quad \mathbf{u} = \mathbf{u}_0 \quad \text{at } t = 0,$$

where $\mathbf{g}$ and $\mathbf{u}_0$, respectively, denote a given boundary velocity, tangential to $\partial\Omega_f$, and a given initial flow field in Ω_f.

The current distribution in the entire region Ω is subject to Ohm's law:

$$\mathbf{J} = \sigma(\mathbf{E} + \chi_f\mathbf{u}\times\mathbf{B}) \quad \text{in } \Omega. \tag{2}$$

Here $\mathbf{E}$ denotes the electric field, and χ_f is the characteristic function of the fluid region Ω_f (that is, $\chi_f = 1$ in Ω_f and $\chi_f = 0$ everywhere else). The electrical conductivity σ

is assumed to be constant in each of the conductors involved, but with possibly different values in different conductors. (This assumption could be further relaxed to allow for spatially inhomogeneous and anisotropic solid conductors, where σ would be a symmetric and positive definite tensor function of position.) The total current distribution,

$$\mathbf{J}_{tot} = \mathbf{J} + \mathbf{J}_{ext} = \begin{cases} \mathbf{J} & \text{in } \Omega, \\ \mathbf{J}_{ext} & \text{in } \mathbb{R}^3 \setminus \overline{\Omega}, \end{cases} \tag{3}$$

which may include given, externally maintained currents $\mathbf{J}_{ext}$, must satisfy the continuity equation

$$\nabla \cdot \mathbf{J}_{tot} = 0 \quad \text{in } \mathbb{R}^3. \tag{4}$$

Note that in (3) we identify the vector fields $\mathbf{J}$ and $\mathbf{J}_{ext}$ with their respective zero extensions to $\mathbb{R}^3$. Assuming $\mathbf{J}_{ext}$ to be solenoidal in $\mathbb{R}^3 \setminus \overline{\Omega}$, Equation (4), which must be interpreted in the sense of distributions on $\mathbb{R}^3$, is equivalent with

$$\nabla \cdot \mathbf{J} = 0 \quad \text{in } \Omega \quad \text{and} \quad \mathbf{J} \cdot \mathbf{n} = \mathbf{J}_{ext} \cdot \mathbf{n} \quad \text{on } \partial\Omega, \tag{5}$$

where $\mathbf{n}$ denotes the outward unit normal vector field on $\partial\Omega$.

The key idea now is to "eliminate" the magnetic and electric fields $\mathbf{B}$ and $\mathbf{E}$ from the equations. To that end, the magnetic field is decomposed as

$$\mathbf{B} = \mathbf{B}_{ext} + \mathcal{B}(\mathbf{J}_{tot}),$$

where $\mathbf{B}_{ext}$ denotes a given, externally generated field while $\mathcal{B}(\mathbf{J}_{tot})$ is the field induced by $\mathbf{J}_{tot}$. The latter satisfies Maxwell's equations (in the quasi-stationary approximation customarily adopted in MHD):

$$\nabla \times \mu^{-1}\mathcal{B}(\mathbf{J}_{tot}) = \mathbf{J}_{tot} \quad \text{and} \quad \nabla \cdot \mathcal{B}(\mathbf{J}_{tot}) = 0 \quad \text{in } \mathbb{R}^3. \tag{6}$$

The magnetic permeability μ is assumed to be constant in each of the media that constitute the region Ω as well as in the exterior of Ω, but with possibly different values in different media. The equations (6) are interpreted in the sense of distributions on $\mathbb{R}^3$; as such they incorporate the jump conditions and continuity relations that $\mathbf{B}$ must satisfy at interfaces separating media of different magnetic permeability.

Next, a magnetic vector potential

$$\mathbf{A} = \mathbf{A}_{ext} + \mathcal{A}(\mathbf{J}_{tot})$$

is introduced. Here $\mathbf{A}_{ext}$ denotes a (given) solenoidal vector potential for $\mathbf{B}_{ext}$ while $\mathcal{A}(\mathbf{J}_{tot})$ is to be determined from

$$\nabla \times \mu^{-1}\nabla \times \mathcal{A}(\mathbf{J}_{tot}) = \mathbf{J}_{tot} \quad \text{and} \quad \nabla \cdot \mathcal{A}(\mathbf{J}_{tot}) = 0 \quad \text{in } \mathbb{R}^3,$$

or equivalently (since $\nabla \cdot \mathbf{J}_{tot} = 0$) from

$$\nabla \times \mu^{-1}\nabla \times \mathcal{A}(\mathbf{J}_{tot}) - \nabla\mu^{-1}\nabla \cdot \mathcal{A}(\mathbf{J}_{tot}) = \mathbf{J}_{tot} \quad \text{in } \mathbb{R}^3. \tag{7}$$

Under mild assumptions on $\mathbf{J}_{tot}$, this equation admits a unique solution vanishing at infinity. In fact, Equation (7) permits the consistent definition of vector fields $\mathcal{A}(\mathbf{K})$ and

$\mathcal{B}(\mathbf{K})$ even for not necessarily solenoidal distributions $\mathbf{K}$: Let $\mathcal{A}(\mathbf{K})$ denote the unique solution of

$$\nabla \times \mu^{-1} \nabla \times \mathcal{A}(\mathbf{K}) - \nabla \mu^{-1} \nabla \cdot \mathcal{A}(\mathbf{K}) = \mathbf{K} \quad \text{in } \mathbb{R}^3 \quad \text{and} \quad \mathcal{A}(\mathbf{K}) = 0 \quad \text{at } \infty$$

and set $\mathcal{B}(\mathbf{K}) = \nabla \times \mathcal{A}(\mathbf{K})$. Although neither $\mathbf{J}$ nor $\mathbf{J}_{ext}$ are solenoidal as distributions on $\mathbb{R}^3$ (unless $\mathbf{J} \cdot \mathbf{n} = \mathbf{J}_{ext} \cdot \mathbf{n} = 0$ on $\partial\Omega$), the magnetic field can now be further decomposed as

$$\mathbf{B} = \mathbf{B}_0 + \mathcal{B}(\mathbf{J}) \quad \text{with} \quad \mathbf{B}_0 = \mathbf{B}_{ext} + \mathcal{B}(\mathbf{J}_{ext})\,. \tag{8}$$

To obtain a similar decomposition for the electric field, the same is written as

$$\mathbf{E} = \mathbf{E}_{ext} + \mathcal{E}(\mathbf{B})\,,$$

where $\mathbf{E}_{ext}$ denotes a given, externally generated field while $\mathcal{E}(\mathbf{B})$ is the field induced by the time variation of $\mathbf{B}$. The latter obeys Faraday's law:

$$\nabla \times \mathcal{E}(\mathbf{B}) = -\mathbf{B}_t \quad \text{in } \mathbb{R}^3.$$

Since $\mathbf{B} = \nabla \times \mathbf{A}$, there exists a scalar potential ϕ (on $\mathbb{R}^3$) such that $\mathcal{E}(\mathbf{B}) + \mathbf{A}_t = -\nabla\phi$, and it follows that

$$\mathbf{E} = \mathbf{E}_0 - \mathcal{A}(\mathbf{J}_t) - \nabla\phi \quad \text{with} \quad \mathbf{E}_0 = \mathbf{E}_{ext} - \mathbf{A}_{ext,t} - \mathcal{A}(\mathbf{J}_{ext,t})\,. \tag{9}$$

Substitution of (8) and (9) into Ohm's law (2) yields

$$\mathcal{A}(\mathbf{J}_t) + \sigma^{-1}\mathbf{J} + \nabla\phi - \chi_f \mathbf{u} \times \big(\mathbf{B}_0 + \mathcal{B}(\mathbf{J})\big) = \mathbf{E}_0 \quad \text{in } \Omega.$$

The above constitutes an evolution equation for the unknown current density $\mathbf{J}$, in which the scalar potential ϕ plays the role of a Lagrange multiplier associated with the divergence constraint $\nabla \cdot \mathbf{J} = 0$, in complete analogy to the role of the pressure p in the Navier-Stokes equations (1). A boundary condition for $\mathbf{J}$ is already contained in (5):

$$\mathbf{J} \cdot \mathbf{n} = j \quad \text{on } \partial\Omega \quad \text{where} \quad j = \mathbf{J}_{ext} \cdot \mathbf{n}\,.$$

All that is needed to close the system of equations is an initial condition for $\mathbf{J}$,

$$\mathbf{J} = \mathbf{J}_0 \quad \text{at } t = 0,$$

where $\mathbf{J}_0$ denotes a given initial current distribution in Ω.

In summary, the following initial-boundary value problem must be solved for the velocity, pressure, current density, and electric potential:

$$\rho\mathbf{u}_t - \eta\Delta\mathbf{u} + \rho(\mathbf{u}\cdot\nabla)\mathbf{u} + \nabla p - \mathbf{J} \times \big(\mathbf{B}_0 + \mathcal{B}(\mathbf{J})\big) = \mathbf{F}_0 \quad \text{and} \quad \nabla \cdot \mathbf{u} = 0 \quad \text{in } \Omega_f, \tag{10}$$

$$\mathbf{u} = \mathbf{g} \quad \text{on } \partial\Omega_f \quad \text{and} \quad \mathbf{u} = \mathbf{u}_0 \quad \text{at } t = 0, \tag{11}$$

$$\mathcal{A}(\mathbf{J}_t) + \sigma^{-1}\mathbf{J} + \nabla\phi - \chi_f \mathbf{u} \times \big(\mathbf{B}_0 + \mathcal{B}(\mathbf{J})\big) = \mathbf{E}_0 \quad \text{and} \quad \nabla \cdot \mathbf{J} = 0 \quad \text{in } \Omega, \tag{12}$$

$$\mathbf{J} \cdot \mathbf{n} = j \quad \text{on } \partial\Omega \quad \text{and} \quad \mathbf{J} = \mathbf{J}_0 \quad \text{at } t = 0, \tag{13}$$

$$\text{where} \quad \mathcal{B}(\mathbf{J}) = \nabla \times \mathcal{A}(\mathbf{J}) \quad \text{and}$$

$$\nabla \times \mu^{-1} \nabla \times \mathcal{A}(\mathbf{J}) - \nabla \mu^{-1} \nabla \cdot \mathcal{A}(\mathbf{J}) = \mathbf{J} \quad \text{in } \mathbb{R}^3 \quad \text{and} \quad \mathcal{A}(\mathbf{J}) = 0 \quad \text{at } \infty. \tag{14}$$

Note that if μ is constant throughout space, then (14) reduces to

$$-\Delta\mathcal{A}(\mathbf{J}) = \mu\mathbf{J} \quad \text{in } \mathbb{R}^3 \quad \text{and} \quad \mathcal{A}(\mathbf{J}) = 0 \quad \text{at } \infty,$$

in which case

$$\mathcal{A}(\mathbf{J}) = \frac{\mu}{4\pi}\int_\Omega \frac{\mathbf{J}(y)}{|x-y|}\,dy$$

(the Newtonian potential of $\mathbf{J}$) and

$$\mathcal{B}(\mathbf{J}) = -\frac{\mu}{4\pi}\int_\Omega \frac{x-y}{|x-y|^3} \times \mathbf{J}(y)\,dy \tag{15}$$

(the Biot-Savart formula for the magnetic field induced by $\mathbf{J}$). In general, when integral representations for $\mathcal{A}(\mathbf{J})$ and $\mathcal{B}(\mathbf{J})$ are unavailable or inconvenient, Equation (14) must be solved simultaneously with (10)–(13).

It is worth recalling that in the above formulation of the MHD equations, Maxwell's equations are implicitly solved on all of space (except that an extra equation would be needed to determine the electric potential ϕ in the exterior of Ω). In particular, no boundary conditions are imposed on electric and magnetic fields, and the electromagnetic interaction of the conductors in Ω with the surrounding space is fully accounted for.

Of course, it is possible and useful to generalize the boundary conditions in (11) and (13). For example, one could specify the *stress* rather than the velocity on all or part of $\partial\Omega_f$, or alternatively, normal velocity and tangential stress or tangential velocity and normal stress. Also, one could specify the *electric potential* rather than the current flux on all or part of $\partial\Omega$. Under such generalized boundary conditions, however, the electromagnetic interaction between Ω and its exterior would be partially neglected. Suppose, for example, that the electric potential is specified on parts of $\partial\Omega$, modeling the presence of electrodes by means of which a current is passed through the configuration. Obviously, a supply current must be provided to the electrodes in order to maintain the specified potential. The supply current induces magnetic field and, if time-dependent, also electric field; these fields could affect the velocity and current distribution everywhere in Ω. Usually, the effect will be negligible; if it is not, the external wires carrying the supply current should be considered part of Ω, the region of unknown current density.

For a detailed mathematical analysis of the initial-boundary value problem (10)–(14), the reader is referred to a forthcoming publication, where the existence of weak solutions is proved via the Faedo-Galerkin method; [12] deals with a special case. The paper [13] is devoted to the numerical analysis and finite-element approximation of a *stationary* MHD flow problem, under much less general assumptions but based on the same ideas. There, the reader will find a weak formulation of the problem, suitable for finite-element discretization, along with rigorous error estimates, remarks on a specific implementation of the method, and a discussion of several computational experiments.

Application: Flow Around a Spherical Inclusion

Returning to the problem of electromagnetic filtration, as discussed in the introduction, we now consider the stationary flow of an electrically conducting fluid (of density ρ, viscosity η, and conductivity σ_f), confined to a cubic vessel Ω, around a solid spherical particle Ω_p (of conductivity σ_p), located at the center of Ω. In this case, $\Omega_f = \Omega \setminus \overline{\Omega_p}$ and $\sigma = \sigma_f$ in Ω_f, $\sigma = \sigma_p$ in Ω_p. Two opposite faces of the cube Ω are endowed with electrodes, held at constant potentials ϕ_+ and ϕ_-, respectively, and a steady, uniform magnetic field $\mathbf{B}_0$ is applied perpendicular to the ensuing electric field and current.

No further external forcing is considered ($\mathbf{F}_0 = 0$, $\mathbf{E}_0 = 0$), and no external currents are accounted for ($\mathbf{J}_{ext} = 0$). The boundary conditions are $\mathbf{u} = 0$ on $\partial\Omega_f$ and $\mathbf{J} \cdot \mathbf{n} = 0$ on $\partial\Omega$, except on the two electrodes, where $\phi = \phi_\pm$, respectively. The magnetic permeability μ is assumed to be constant throughout space, so that the induced magnetic field $\mathcal{B}(\mathbf{J})$ can be computed via the Biot-Savart formula (15). The problem being stationary, the vector potential $\mathcal{A}(\mathbf{J})$ is not needed here.

To obtain a finite-element discretization of the problem, the flow domain Ω_f (a cube with a spherical cavity) is decomposed by first mapping it to a cube with a *cubic* cavity and then decomposing the latter into cubes of equal size. The choice of finite elements is the same as in [13]: continuous piecewise triquadratics for the velocity components and the electric potential; continuous piecewise trilinears for the pressure; and gradients of continuous piecewise triquadratics for the current density (the latter is a somewhat nonstandard choice, dictated by a well-known stability condition). In view of the error estimates in [13], the discretization error is expected to be of order h^2 (where h is the grid size).

The nonlinear system of algebraic equations resulting from the finite-element discretization is solved with a simple linearization/iteration scheme, in which the first variable of the inertia term $(\mathbf{u} \cdot \nabla)\mathbf{u}$ and the induced magnetic field $\mathcal{B}(\mathbf{J})$ are lagged behind. At each step of the iteration, $\mathcal{B}(\mathbf{J})$ is computed via Gaussian quadrature of the Biot-Savart integral (15). Since $\mathcal{B}(\mathbf{J})$ is lagged behind, the nonlocal nature of the operator $\mathcal{B}$ does not destroy the sparsity of the resulting linear-algebraic systems. Those are solved directly.

We simulated the flow in two typical albeit academic situations, with $\sigma_p = 10\sigma_f$ and $\sigma_p = 0.1\sigma_f$, respectively. All parameters (except for σ_p) were set equal to 1. The domain Ω was a unit cube centered at the origin, Ω_p a sphere of radius 0.1. The electrodes, located at $x = \pm 0.5$, were held at potentials $\phi_\pm = \pm 1$, respectively, and the applied magnetic field, in the z-direction, had magnitude 10. For both cases, $\sigma_p = 10\sigma_f$ and $\sigma_p = 0.1\sigma_f$, Table 1 lists the computed Lorentz, pressure, viscous, and resultant forces acting on the particle, that is, the x-, y-, and z-components of

$$\mathbf{F}_L = \int_{\Omega_p} \mathbf{J} \times \mathbf{B}\,, \quad \mathbf{F}_P = -\int_{\partial\Omega_p} p\,\mathbf{n}\,, \quad \mathbf{F}_V = \eta \int_{\partial\Omega_p} \big(\nabla\mathbf{u} + (\nabla\mathbf{u})^T\big)\mathbf{n}\,,$$

and

$$\mathbf{F}_R = \mathbf{F}_L + \mathbf{F}_P + \mathbf{F}_V\,.$$

σ_p	$\mathbf{F}_L$	$\mathbf{F}_P$	$\mathbf{F}_V$	$\mathbf{F}_R$
$10\sigma_f$	$+3.679E{-}08$ $+2.007E{-}01$ $+3.518E{-}04$	$+1.605E{-}16$ $-7.880E{-}02$ $-1.422E{-}05$	$+2.150E{-}07$ $-2.922E{-}03$ $-1.318E{-}05$	$+2.518E{-}07$ $+1.190E{-}01$ $+3.244E{-}04$
$0.1\sigma_f$	$+3.630E{-}09$ $+1.556E{-}02$ $+8.298E{-}06$	$+1.613E{-}16$ $-5.497E{-}02$ $-2.586E{-}05$	$+2.339E{-}07$ $+2.501E{-}03$ $-3.084E{-}06$	$+2.339E{-}07$ $-3.691E{-}02$ $-2.065E{-}05$

Table 1. Forces on Particle.

As expected, $\mathbf{F}_L$ acts mostly along the positive y-axis, $\mathbf{F}_P$ along the negative y-axis; $\mathbf{F}_V$ is also strongest in the y-direction, but generally small compared to $\mathbf{F}_L$ and $\mathbf{F}_P$. The resultant force $\mathbf{F}_R$ would cause the particle to migrate in the positive y-direction if $\sigma_p = 10\sigma_f$, in the negative y-direction if $\sigma_p = 0.1\sigma_f$. Figures 1 and 2 (at the end of the paper) depict the current distribution and induced flow field in the case $\sigma_p = 10\sigma_f$.

To illustrate the relative importance of *induction effects*, we repeated both simulations, this time neglecting the induced magnetic field $\mathcal{B}(\mathbf{J})$ (this is easily achieved by setting $\mu = 0$). The resulting current distributions and flow fields were practically indistinguishable from those obtained earlier, and so were the (relatively large) y-components of the forces experienced by the particle. Noticeable deviations were observed only in the (relatively small) x- and z-components of the forces (see Table 2). This is in line with expectations since the applied magnetic field was roughly one order of magnitude stronger than the induced field. — More systematic flow simulations, involving metallurgically realistic flow parameters and data, are under way and will be discussed elsewhere.

σ_p	$\mathbf{F}_L$	$\mathbf{F}_P$	$\mathbf{F}_V$	$\mathbf{F}_R$
$10\sigma_f$	$+3.499E-08$ $+2.007E-01$ $+0.000E-00$	$+1.613E-16$ $-7.879E-02$ $-9.051E-06$	$+1.925E-07$ $-2.921E-03$ $+2.747E-07$	$+2.275E-07$ $+1.190E-01$ $-8.776E-06$
$0.1\sigma_f$	$+3.392E-09$ $+1.556E-02$ $+0.000E-00$	$+6.465E-07$ $-5.497E-02$ $+7.111E-06$	$+2.172E-07$ $+2.501E-03$ $+8.527E-08$	$+8.637E-07$ $-3.691E-02$ $+7.196E-06$

Table 2. Forces on Particle, with Induction Effects Neglected.

References

1. J.-L. Meyer et al., "Steady Flow of Liquid Aluminum in a Rectangular-Vertical Ingot Mold, Thermally or Electromagnetically Activated," Metall. Trans. B, 15B (1984), 471–478.
2. Ch. Vivès and R. Ricou, "Fluid Flow Phenomena in a Single Phase Coreless Induction Furnace," Metall. Trans. B, 16B (1985), 227–235.
3. P.J. Prescott and F.P. Incropera, "Magnetically Damped Convection During Solidification of a Binary Metal Alloy," J. Heat Transfer (Trans. ASME), 115 (1993), 302–310.
4. J. Sakane, B.Q. Li, and J.W. Evans, "Mathematical Modeling of Meniscus Profile and Melt Flow in Electromagnetic Casters," Metall. Trans. B, 19B (1988), 397–408.
5. Ch. Vivès and R. Ricou, "Liquid-Solid Separation in a Molten Metal by a Stationary Electromagnetic Field," Liquid-Metal Flows and Magnetohydrodynamics, ed. H. Branover, P.S. Lykoudis, and A. Yakhot (New York, NY: AIAA, 1983), 387–401.
6. Ph. Marty et al., "Pressure and Velocity Distribution Around an Obstacle Immersed in Liquid Metal Subjected to Electromagnetic Forces," in Ref. 5, 402–413.
7. N. El-Kaddah, A.D. Patel, and T.T. Natarajan, "The Electromagnetic Filtration of Molten Aluminum Using an Induced-Current Separator," JOM, 47 (5) (1995), 46–49.
8. G. Gerbeth, A. Thess, and P. Marty, "Theoretical Study of the MHD Flow Around a Cylinder in Crossed Electric and Magnetic Fields," Eur. J. Mech. B Fluids, 9 (3) (1990), 239–257.
9. A.D. Patel and N. El-Kaddah, "On the MHD Flow Around a Non-conducting Spherical Droplet in Crossed Electric and Magnetic Fields," Eighth Beer-Sheva International Seminar on Magnetohydrodynamic Flows and Turbulence (Beer-Sheva, Israel: Ben-Gurion University of the Negev, 1996).
10. N. El-Kaddah, "Analytical and Numerical Analysis of the MHD Flow Around a Sphere in Crossed Electric and Magnetic Fields" (Paper presented at the 1998 SIAM Annual Meeting, Toronto, Canada, July 13–17, 1998).
11. A.D. Patel and N.H. El-Kaddah, "On the Theory of Electromagnetic Separation in Alternating Electromagnetic Fields," International Symposium on Electromagnetic Processing of Materials (Nagoya, Japan: ISIJ, 1994), 115–120.
12. P.G. Schmidt, "A Galerkin Method for Time-dependent MHD Flow with Nonideal Boundaries," Comm. Appl. Anal. (to appear).
13. A.J. Meir and P.G. Schmidt, "Analysis and Numerical Approximation of a Stationary MHD Flow Problem with Nonideal Boundary," SIAM J. Numer. Anal. (to appear).

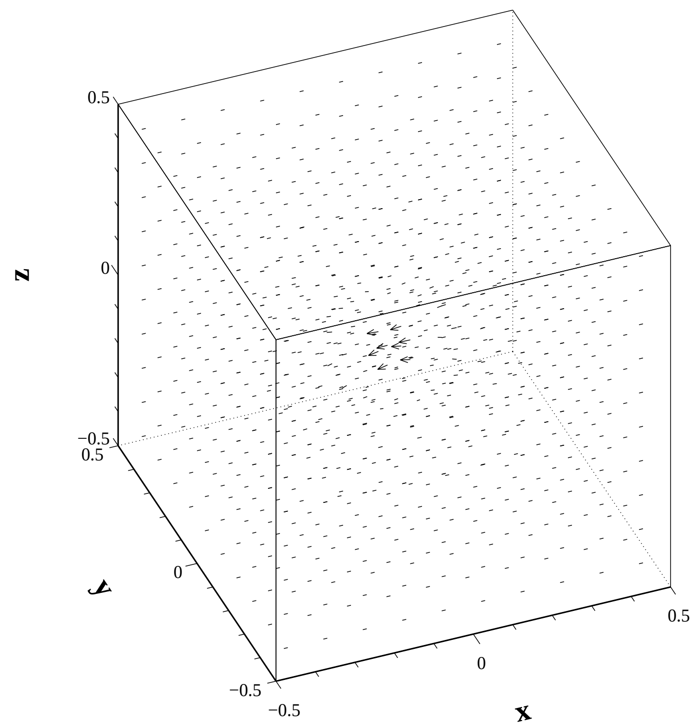

Figure 1. Current Distribution for $\sigma_p = 10\sigma_f$.

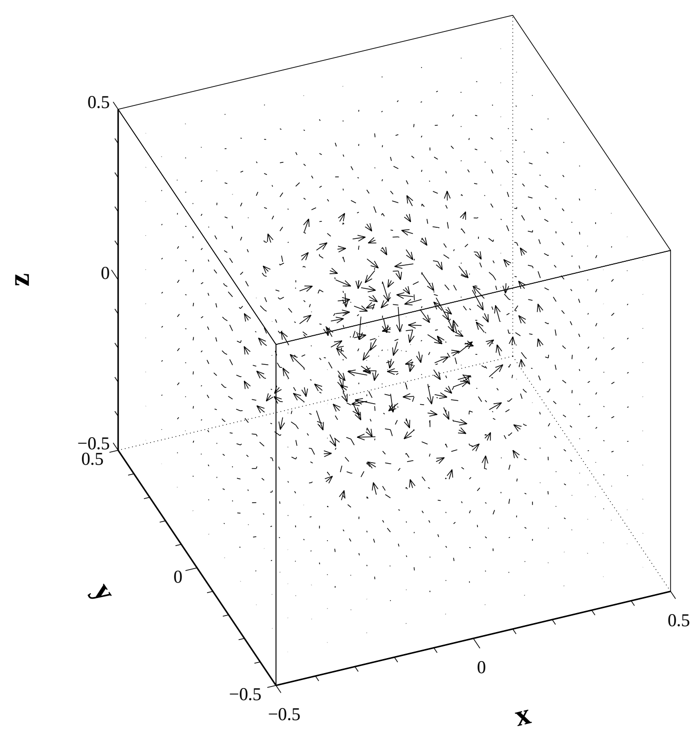

Figure 2. Velocity Field for $\sigma_p = 10\sigma_f$.